MDPI

Article

Characterizing forest spatial heterogeneity using UAV LiDAR and dimensional differentiation indices

Nicola Puletti[1], Matteo Guasti[1], Simone Innocenti[1], Lorenzo Cesaretti[1,2] and Ugo Chiavetta[1]

[1] Research Centre for Forestry and Wood, CREA
[2] Civil, Constructional and Environmental Engineering, Sapienza University
* Correspondence: nicola.puletti@crea.gov.it

Abstract: Understanding the heterogeneity of vertical structure of forests is essential for understanding ecosystem dynamics, biodiversity conservation, and sustainable forest management. Unmanned Aerial Vehicle (UAV) LiDAR technology offers a promising approach to capture detailed three-dimensional (3D) information about forest canopies at company level. In this study, we present an investigation into the heterogeneity of vertical forest structure in broadleaf forests utilizing UAV LiDAR data. Through comprehensive data analysis techniques proposed, including point cloud segmentation and statistical metrics based on leaf area density profiles, we described vertical variability of managed beech forests. Our findings highlight the significance of UAV LiDAR in characterizing the complexity and variability of forest vertical structure at high resolution, offering valuable insights for biodiversity conservation, carbon accounting, and sustainable forest management practices. We seek to explore not only the vertical heterogeneity but also the spatial arrangement of vegetation elements within managed Beech forests.

Keywords: precision forestry; vertical profile traits; managed forests; broadleaf forests

Citation: Puletti, N.; Guasti, M.; Innocenti, S.; Cesaretti, L.; Chiavetta, U. Characterizing forest spatial heterogeneity using UAV LiDAR and dimensional differentiation indices . *Remote Sens.* **2024**, *1*, 0. https://doi.org/

Received:
Revised:
Accepted:
Published:

1. Introduction

Light is among the major factors affecting tree growth, and tree crowns play a fundamental role in determining the amount of light and the microclimatic conditions experienced by all living organisms in forest ecosystems [1]. Crown size and shape influence various aspects of tree life, such as growth, mortality, stability, and reproductive success, consequently impacting the overall dynamics of the entire forest [2]. These features greatly depend on the spatial arrangement resulting from species-specific strategies, like lateral extension for light capture, maintenance of mechanical stability and hydraulic safety, and growth speed (i.e. slow versus fast growth) [3,4]. Beside these traits, forest management plays a central role. Predicting crown competition effects is crucial not only for ecological studies on natural forests but also for the economy of managed stands. A strong competition can indeed diminish the yield and vigor of single trees and potentially leading to their suppression and death.

Plenty of scientific literature grounds its results on simplified and geometric representations of crown features, appealing to our natural preference for schematization in understanding patterns and processes in nature [5]. However, numerous empirical studies indicate that variability in crown structure, rather than uniformity, is crucial for a tree's success in dealing with competition [6]. Even in stands with uniform canopy height, competition for canopy space and light is much more likely to be markedly asymmetric rather than quasi-symmetric. The heterogeneous distribution of light in the canopy, caused by partial

shading from neighbors, results in some canopy sections experiencing slow growth while well-lit regions exhibit vigorous expansion. Trees exhibit plastic modifications of their canopy structure as a powerful response to these heterogeneous light conditions. They grow toward areas with higher light availability and reduced competition, thereby avoiding neighbors. Due to this morphological plasticity, tree canopies are rarely positioned directly above the stem base [7]. All these elements lead to asymmetric canopy growth.

The so-called "neighborhood approach" is the basis of all studies that investigate small-scale tree-tree competition between trees of different sizes and/or different species [7,8]. Following this approach, (a) the identification of neighbors having an actual effect on focal tree and (b) a suitable selection of crown traits (for both k-neighbors and j-focal trees), are crucial steps. With some exceptions (e.g. Winkelmass, also known as uniform angle index, for which k is 4 [8–10]), spatial indices are very flexible in the number of neighbor trees.

The identification of neighbors with potential effects on focal tree is usually based on the position of the dbh [10,11]. Nevertheless, the real tree-tree competition is at the rooth and crown level: the growth in dbh is only a reflection of how much plants accumulate in terms of water and light. Accurate measurement of tree crown features is therefore essential to better understand competition [7]. However, traditional methods for their precise measurement have limitations. Tools such as calipers (for diameters at breast height (dbh)), tapes (for crown projections) and, recently, laser/sonar range finder (for total tree heights) are very time-consuming for 3D accurate measures and are subject to non-negligible positioning errors.

More recent is the use of terrestrial laser scanners [TLS, 12]. In that case, limitations arise in mature or even-aged forest stands, where the upper part of the canopy cannot be seen by the scanner, even in leaf-off conditions. The recent introduction of miniaturized LiDAR instruments, mountable on unmanned aerial systems (UAV-LS), and GPS-RTK positioning systems, overcome these constrains, allowing precise point clouds co-registrations [13].

In the present study, we focused on evaluate the potential of UAV-LS to describe crown-crown features in a pure Beech managed forest in Central Italy. Specific objectives are: (1) present a new semi-automatic and dynamic method for effective tree-neighbors selection. (2) Obtain detailed crown projected area, and crown volume. (3) Evaluate the differences between DBH differentiation index calculated using fixed or dynamic number of neighbors and dimensional differentiation index [14] for both crown projected area, crown volume, and tree volume.

To do this, we used a set of Beech trees manually detected from co-registered TLS and UAV-LS data and analyzed following an approach recently introduced by ecologists on TLS data only [15]. TLS data, acquired simultaneously to UAV-LS, were used as reference for tree stem positioning and traditional indices calculations. We defined competitor - i.e. trees that are likely to impose competitive pressures on a focal tree - all those surrounding trees that were part of the upper canopy layer and were in direct contact with the crown of the focal tree [as for 7].

2. Materials

This study was conducted in Alpe di Catenaia, Italy. Data were collected in October-December 2023 (circular sampling plots, 15 m radius) in pure Beech forest stands with similar climate conditions, soil types, forest structure, and management history [13]. Sampling plots were placed in the study area following a spatially balanced approach [16].

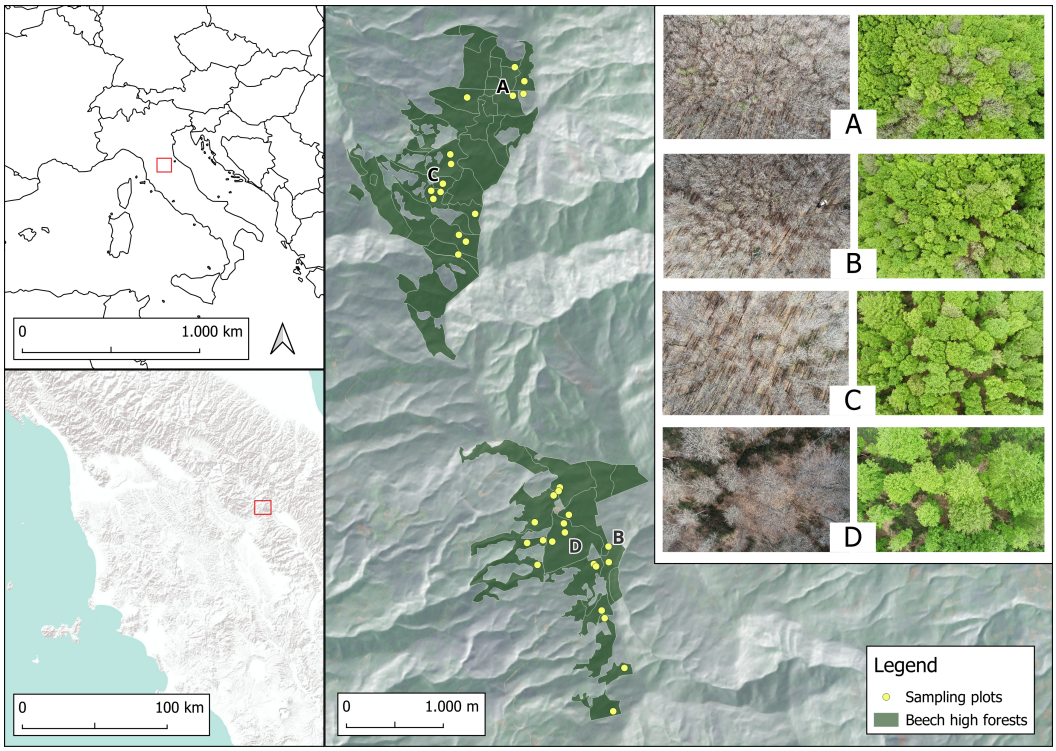

Figure 1. study area

TLS-inventory measurements were performed by GeoSLAM ZEB-REVO (GeoSLAM Ltd., Ruddington, England) lightweight mobile laser scanner. It features a rotating 2D scanning device and an inertial measurement unit in the handle. The system acquires 3D information of the sur- rounding area through measurements, due to the motion offered by the scanning head on the motor drive, enabling the application of 3D-simultaneous location and mapping algorithms [17]. This TLS requires that the starting and ending points of the scan process coincide and some overlaps are done during the scan path. The center of the plot was georeferenced using a RTK GPS.

We collected UAV LiDAR (UAV-LS) data across simultaneously to TLS measurements on the field. The UAV-LS LiDAR platform consisted of a DJI Matrice 350 quadcopter integrated with Zenmuse L1 LiDAR sensor (DJI Inc. in Shenzhen, China), an advanced scanning sensor designed for aerial surveying applications. It integrates a LiDAR module, an RGB camera with a non-full-frame configuration, and an inertial measurement unit (IMU). With a detection range of 450 m under 80% reflectivity conditions, a high point rate of up to 240,000 points per second and ranging accuracy of 3 cm at a range of 100 m [18,19].

The flights were performed at approximately 55 m above the digital terrain model uploaded on UAV-LS, with approximately 13 km h^{-1} speed. With these settings, the resulting point cloud has a mean point density of about 1500 points m^{-2}. Data processing was done in Terra® software which allowed us to bring in the trajectory data of the drone flight, align the flight paths, georeference the point cloud and then export it in LAS format.

Both TLS and UAV-LS data were collected during leaf-off phenological phase. Every point cloud was clipped by corresponding 15 m radius circles and co-registered using Cloud Compare [20] following the procedure described in a previous work [13].

3. Methods

From the co-registered point cloud, we manually segmented a total of 299 trees (115 of which are focal trees), producing Quantitative Structure Models (QSMs). For each tree we

derived tree XY-position and diameter at breast height (dbh, Figure 2), total tree height (TH), total tree volume (Tvol) and 3 crown features (see Section 3.1).

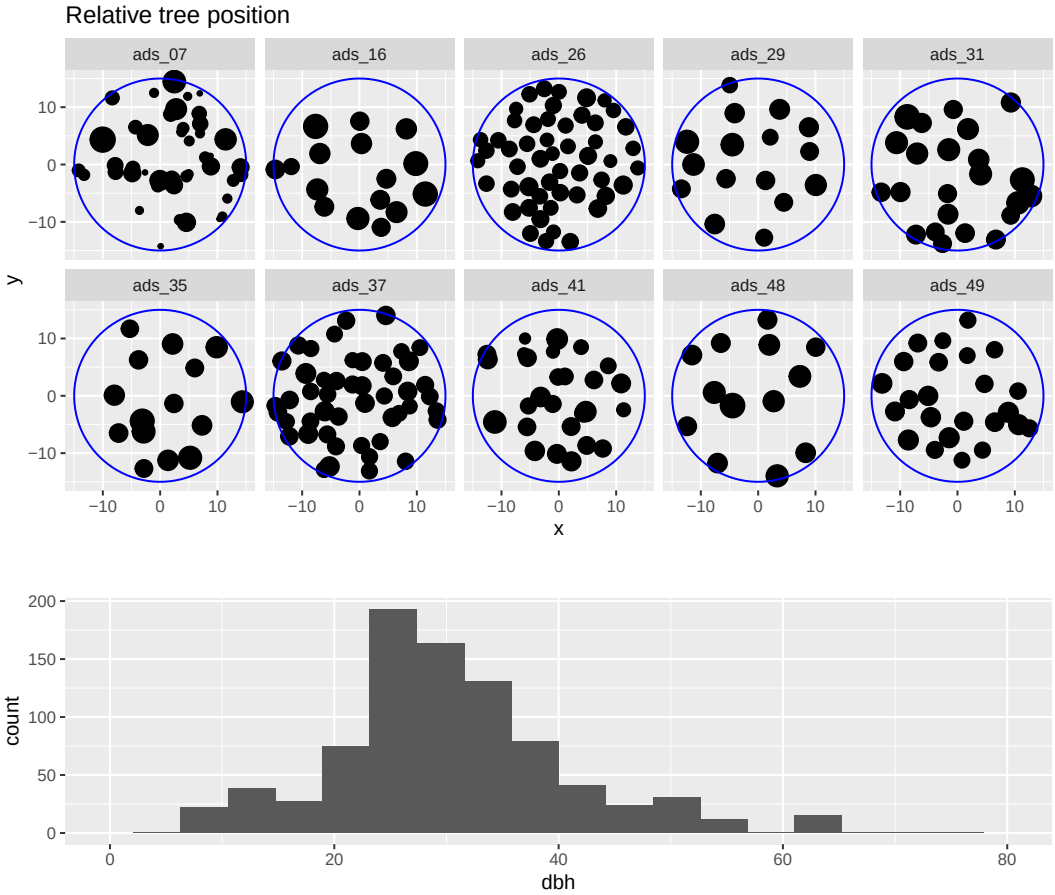

Figure 2. On the top: Tree positions for sampling plots considered in this study. Point size is proportional to dbh. Below: histogram of dbh distribution for trees measured.

3.1. Crown features

As crown features we computed: crown projected area (CrPrj), the XY-position of its centroid (xyCnt) and crown volume (CrVol). Using the lidR package (Roussel et al. [21]), we created a set of algorithms that allowed to parameterize various structural crown attributes from the xyz-data of each focal tree and its neighbors. To do so, the single tree original point cloud (Figure 3, on the left) was first voxelized at a resolution of 25 cm (Figure 3), a good compromise for fast computation with a mid-to-high performance hardware. To avoid the residual noise in the original point cloud, only voxels with at least 3 points were considered as "vegetation" and used to compute single tree vertical profiles. From its smoothed curve (red-line in Figure 3) we derived the height of the maximum crown projection (Z peak, in meters), crown base height (Z peak start, in meters) and total tree height (Z peak end, in meters). Crown volume (CrVol) was computed as the sum of all vegetation voxels between Z peak start and Z peak end (Figure 3, dark-grey voxels in the center), while crown projected area (CrPrj) was calculated using a 2D convex hull (Figure 3, bottom-right).

3.2. Differentiation dimensional indices

Dimensional differentiation indices can be calculated by applying the following formula:

$$T_X = 1 - \frac{1}{n}\sum_{k=1}^{n}\frac{min(X_i, X_k)}{max(X_i, X_k)} \quad (1)$$

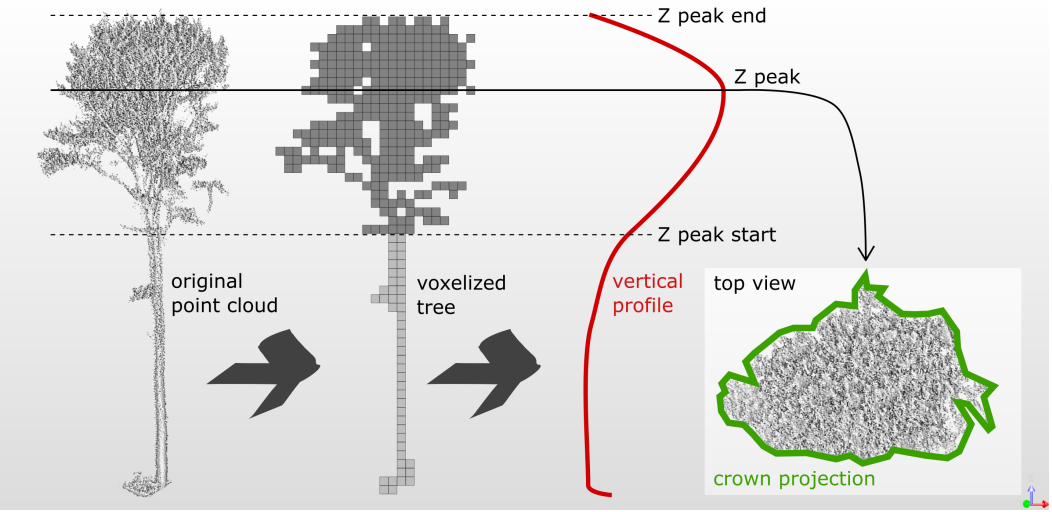

Figure 3. Left: three-dimensional point cloud of a single tree as created by the UAV-LS. Center: voxel-based representation of the same tree. Red-line on the right: smoothed vertical profile of the same tree. Bottom-right in green: convex hull polygon of crown projection at the 'Z peak' height.

were X_i and X_k are the tree-dimensional variable of interest of focal and surrounding trees, respectively [14]. For example, if we are interested in evaluating competition in diameter, following Equation 1, the DBH differentiation index [9] can be calculated as:

$$T_4 = 1 - \frac{1}{n}\sum_{k=1}^{n}\frac{min(DBH_i, DBH_k)}{max(DBH_i, DBH_k)} \tag{2}$$

the number of nearest trees is usually a fixed number, frequently 4, i.e. the nearest trees in terms of DBH XY-position (Keren et al. [22]). Since tree-tree competition for light starts from canopy, in this study we proposed a dynamic neighbors selection considering crown position (Figure 4). In summary, starting from the crown centroid of the focal tree, we selected the nearest trees following an angular searching method, in order to detect the nearest trees from all directions. For details see Figure 4's caption.

We then compared results between five different dimensional indices: (a) DBH differentiation index with k=4 (T_4, Equation 2); (b) DBH differentiation index with k nearest crowns (T_d, Equation 3); (c) crown projection differentiation index (T_{CrPrj}, Equation 4); (d) crown volume differentiation index (T_{CrVol}, Equation 5); (e) tree volume differentiation index (T_{vol}, Equation 6).

$$T_d = 1 - \frac{1}{n}\sum_{k=1}^{n}\frac{min(dbh_i, dbh_k)}{max(dbh_i, dbh_k)} \tag{3}$$

$$T_{CrPrj} = 1 - \frac{1}{n}\sum_{k=1}^{n}\frac{min(CrPrj_i, CrPrj_k)}{max(CrPrj_i, CrPrj_k)} \tag{4}$$

$$T_{CrVol} = 1 - \frac{1}{n}\sum_{k=1}^{n}\frac{min(CrVol_i, CrVol_k)}{max(CrVol_i, CrVol_k)} \tag{5}$$

$$T_{vol} = 1 - \frac{1}{n}\sum_{k=1}^{n}\frac{min(vol_i, vol_k)}{max(vol_i, vol_k)} \tag{6}$$

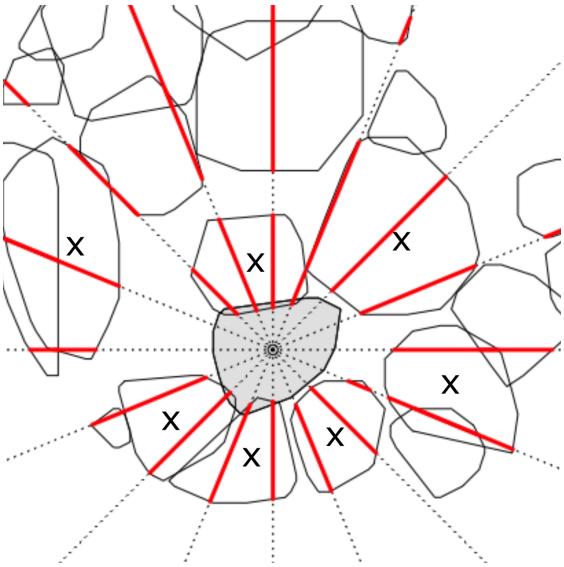

Figure 4. Proposed neighbors' selection for a focal tree (in grey). Starting from crown centroid, the algorithm sketches 16 half-lines dividing the round-angle in 16 equal angles of 22.5° each. A neighbor crown is selected if one of 16 half-lines intersect it (red lines). As final step, only nearest intersected crowns in the same half-line were selected as neighbor tree (marked with a "X" in the figure).

3.3. Statistical analysis

We tested all calculated indices for normality with the Shapiro–Wilk test. Where indices exhibited non-normal frequency distributions and/or heteroscedasticity, multiple paired Wilcoxon tests were conducted to determine the index values that differed significantly. All statistical tests were conducted at $= 0.05$. Data analysis was performed in the R statistical package, Version 4.2.3 (Team [23]).

4. Results

4.1. Segmentation

The time required to create the reference dataset depends, as expected, on the complexity of the forest stand. In total, 18 person-days were needed to isolate and measure the beech trees from which the 115 focal trees and their respective neighbors were selected, with an average of 1.8 days per sampling plot. The duration of this phase mainly depends on the size of the trees.

4.2. Tree features descriptive statistics

Diametro (medio, min, max e sd), altezza (medio, min, max, sd), volume degli alberi (medio, min, max, sd), proiezioni (medio, min, max, sd) e volumi di chioma (medio, min, max, sd).

4.3. Indices statistic analysis

All the indices exhibited non-normal frequency distribution. Table 1 shows the two-sample Wilcoxon test results (with Bonferroni correction for multiple comparisons).

Table 1. p-values of the two-sample Wilcoxon test (with Bonferroni correction for multiple comparisons) for all possible pairs among the considered indices.

	T_d	T_4	T_{CrPrj}	T_{CrVol}
T_4	1			
T_{CrPrj}	7.6e-19	2.73e-18		
T_{CrVol}	3.89e-18	1.47e-17	0.19	
T_{vol}	1.39e-17	1.43e-17	1.69e-04	0.62

The statistical analysis showed that the index based on dbh, calculated using a dynamic number of neighbors (T_d, mean = 0.21; sd = 0.11), yielded almost the same index values as when four neighbor dbh were used (T_4, mean = 0.20; sd = 0.12), although the DBH differentiation index based on four neighbors (T_4) has slightly lower values than T_d (Figure 5). This result was confirmed by the two-sample Wilcoxon test applied to T_4 and T_d distributions (*p-value* = 1, Table 1).

Both mean values and sd of T_{vol} (mean = 0.38; sd = 0.13) are similar to (but slightly lower than) T_{CrPrj} (mean = 0.42; sd = 0.15) and T_{CrVol} (mean = 0.40; sd = 0.16) but, following Wilcoxon test results from Table 1, they significantly differ from T_4 and T_d (*p-value* always lower than 0.001 for all pairs). Moreover, T_{vol} and T_{CrPrj} showed a significant difference in distribution (*p-value* = 1.69e-04).

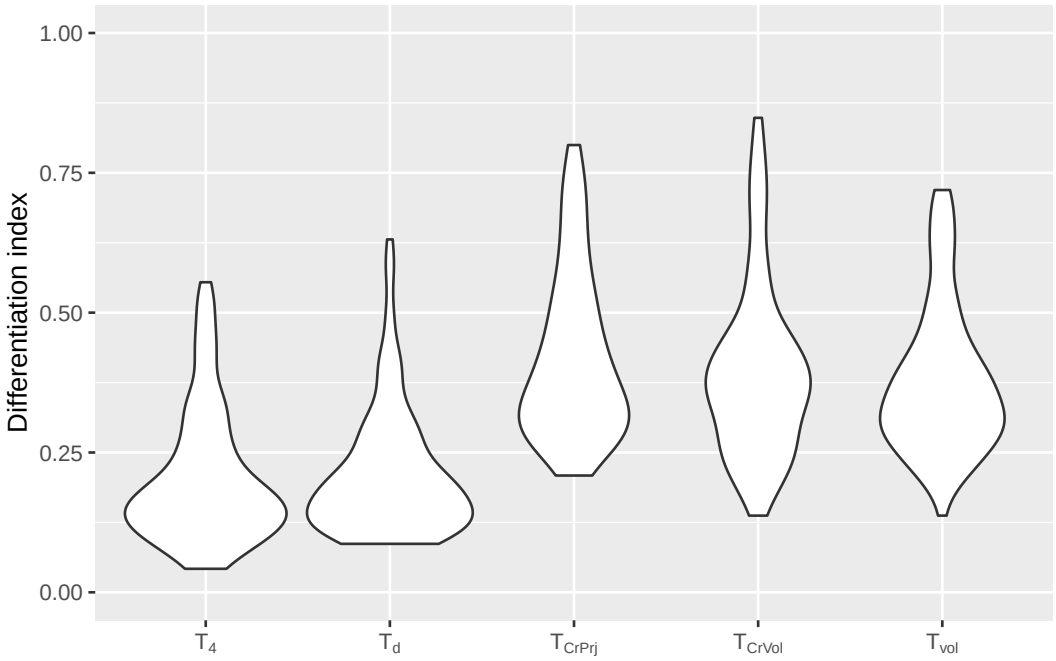

Figure 5. Differences bla bla bla...

5. Discussion and conclusions

Leaf-off scans are essential to identify and position and their structural features in broadleaf forests with accuracy. But although the greater detail provided by UAV-LS, automatic segmentation techniques still represent a major bottleneck in broadleaf forests. Nevertheless, the higher scanning density guaranteed by UAV-LS flights allows a more detailed measure of crown features and spatial arrangement of trees, also in homogeneous stands, like those analysed in this study.

Expanding the knowledge on this topic is important for plenty of reasons [24]. From results obtained in this study, the use of UAV-LS can completely replace the traditional ground-

based approach in measuring tree crowns features, and providing the additional advantage of being able to work over larger areas more efficiently. In summary, this methodology saves time, resources, and also ensures a more extensive and detailed coverage of the forest stands analyzed.

We performed this experiment on pure beech stands. From an ecological point of view, tree species mixture can positively modify the individual tree allometry [6]. However, absence of species mixture is a useful resource for understanding complex competition dynamics due to species functional traits and distinct scaling properties. Furthermore, since the forest stands we considered grow in rainy areas, water supply does not represent a critical issue and the results here presented are not affected by diversion of resources due to different rooting structures and water acquisition strategies [15].

Our results are in line with those from other similar studies [22]. The difference here is on the selection of neighbor trees, but the informational content of structural indices does not significantly depend on the method used to identify the nearest neighbors. In fact, using a fixed or dynamic number of nearest neighbors did not result in significant differences in the distributions of diameter differentiation indices (Figure 5, Table 1). On the contrary, incorporating different crown traits into the heterogeneity index results in varying levels of informational content, offering diverse perspectives on stand complexity. Specifically, using parameters such as diameter, tree volume, and the apparent volume of the canopy in the calculation of diversity indices reveals different levels of heterogeneity. This variance is not only reflected in the average values and their variability but also in the entire distribution of values. By examining these different characteristics, one can gain a more comprehensive understanding of the structural diversity within the forest stand, highlighting the multifaceted nature of its complexity.

Both UAV-LS and TLS methods allow for the sampling of large trees, which are often more challenging to measure using analog or traditional methods such as calipers and vertex hypsometers. As trees age, they tend to alter their height-to-diameter ratios and significantly increase their structural complexity. This complexity is reflected in the intricate relationships between the trunk, branches, and leaves of individual trees. These structural characteristics cannot be fully captured by diameter measurements alone or by quick canopy surveys from the ground. The advanced capabilities of laser technologies enable the detailed assessment of these complex structures, providing a more comprehensive understanding of the tree's architectural traits. Therefore, employing UAV-LS for tree segmentation not only improves the accuracy of measurements, but also enhances the ability to monitor and study the growth patterns and structural changes of larger, older trees. This level of detail is crucial for effective forest management and conservation, ensuring that the unique characteristics and needs of mature trees are adequately addressed in management plans.

A forest survey at a given time is a photography of the stand. In this specific moment, the canopy - the energy center of the tree - indicates its potential for future growth, whereas the diameters reflect the conditions of its past growth. By analyzing the structural properties of tree canopies, it is possible to gain a clearer understanding of the competitive relationships between individual trees. This method provides valuable insights into future growth prospects. When these insights are applied to groups of neighboring trees, they can significantly contribute to the analysis and prediction of the future dynamics of the entire forest stand. Such detailed information allows for a more nuanced understanding of forest ecology and the interactions within it.

As a result, these advanced monitoring approaches offer substantial benefits to forest management and silviculture. They improve the efficiency and effectiveness of management practices by enabling more accurate predictions and better decision-making processes. This holistic approach to monitoring and analysis ensures that forest resources are managed sustainably, supporting both ecological health and economic viability.

Author Contributions: Author roles were classified using the Contributor Role Taxonomy (CRediT; https://credit.niso.org/) as follows: N.P.: Conceptualization, Project administration, Investigation, Supervision, Methodology, Formal analysis, Writing - review and editing

Funding: This research was funded by Agridigit project

Informed Consent Statement: Informed consent was obtained from all subjects involved in the study.

Data Availability Statement: The data presented in this study are publicly available at the Open Science Framework https://osf.io/ak76r/.

Conflicts of Interest: The authors declare no conflict of interest.

References

1. Dial, R.; Bloodworth, B.; Lee, A.; Boyne, P.; Heys, J. The Distribution of Free Space and Its Relation to Canopy Composition at Six Forest Sites **2004**. p. 14. https://doi.org/https://doi.org/10.1093/forestscience/50.3.312.
2. Hildebrand, M.; Perles-Garcia, M.D.; Kunz, M.; Härdtle, W.; Von Oheimb, G.; Fichtner, A. Tree-tree interactions and crown complementarity: The role of functional diversity and branch traits for canopy packing. *Basic and Applied Ecology* **2021**, *50*, 217–227. https://doi.org/10.1016/j.baae.2020.12.003.
3. Verkerk, P.J.; Fitzgerald, J.B.; Datta, P.; Dees, M.; Hengeveld, G.M.; Lindner, M.; Zudin, S. Spatial distribution of the potential forest biomass availability in Europe. *Forest Ecosystems* **2019**, *6*, 5. https://doi.org/10.1186/s40663-019-0163-5.
4. Aalto, I.; Aalto, J.; Hancock, S.; Valkonen, S.; Maeda, E.E. Quantifying the impact of management on the three-dimensional structure of boreal forests. *Forest Ecology and Management* **2023**, *535*, 120885. https://doi.org/10.1016/j.foreco.2023.120885.
5. Pretzsch, H.; Dieler, J. Evidence of variant intra- and interspecific scaling of tree crown structure and relevance for allometric theory. *Oecologia* **2012**, *169*, 637–649. https://doi.org/10.1007/s00442-011-2240-5.
6. Pretzsch, H. The Effect of Tree Crown Allometry on Community Dynamics in Mixed-Species Stands versus Monocultures. A Review and Perspectives for Modeling and Silvicultural Regulation. *Forests* **2019**, *10*, 810. https://doi.org/10.3390/f10090810.
7. Seidel, D.; Leuschner, C.; Müller, A.; Krause, B. Crown plasticity in mixed forests—Quantifying asymmetry as a measure of competition using terrestrial laser scanning. *Forest Ecology and Management* **2011**, *261*, 2123–2132. https://doi.org/10.1016/j.foreco.2011.03.008.
8. Hui, G.; Gadow, K. Das Winkelmaß **2017**.
9. Pommerening, A. Evaluating structural indices by reversing forest structural analysis. *Forest Ecology and Management* **2006**, *224*, 266–277. https://doi.org/10.1016/j.foreco.2005.12.039.
10. Zhang, M.; Wang, J.; Kang, X. Spatial distribution pattern of dominant tree species in different disturbance plots in the Changbai Mountain. *Scientific Reports* **2022**, *12*, 14161. https://doi.org/10.1038/s41598-022-18621-x.
11. Pommerening, A.; Wang, H.; Zhao, Z. Global woodland structure from local interactions: new nearest-neighbour functions for understanding the ontogenesis of global forest structure. *Forest Ecosystems* **2020**, *7*, 22. https://doi.org/10.1186/s40663-020-00224-5.
12. Disney, M. Terrestrial LiDAR: a three-dimensional revolution in how we look at trees. *New Phytologist* **2019**, *222*, 1736–1741. https://doi.org/10.1111/nph.15517.
13. Puletti, N.; Innocenti, S.; Guasti, M. A co-registration approach between terrestrial and UAV laser scanning point clouds based on ground and trees features. *Annals of Silvicultural Research* **2024**, *49*. https://doi.org/10.12899/asr-2513.
14. Szmyt, J.; Korzeniewicz, R. Do natural processes at the juvenile stage of stand development differentiate the spatial structure of trees in artificially established forest stands? *Forest Research Papers* **2014**, *75*, 171–179. https://doi.org/10.2478/frp-2014-0016.
15. Owen, H.J.F.; Flynn, W.R.M.; Lines, E.R. Competitive drivers of interspecific deviations of crown morphology from theoretical predictions measured with Terrestrial Laser Scanning. *Journal of Ecology* **2021**, *109*, 2612–2628. https://doi.org/10.1111/1365-2745.13670.
16. Fattorini, L.; Puletti, N.; Chirici, G.; Corona, P.; Gazzarri, C.; Mura, M.; Marchetti, M. Checking the performance of point and plot sampling on aerial photoimagery of a large-scale population of trees outside forests. *Canadian Journal of Forest Research* **2016**, *46*. https://doi.org/10.1139/cjfr-2016-0013.
17. Puletti, N.; Grotti, M.; Ferrara, C.; Chianucci, F. Lidar-based estimates of aboveground biomass through ground, aerial, and satellite observation: A case study in a Mediterranean forest. *Journal of Applied Remote Sensing* **2020**, *14*. https://doi.org/10.1117/1.JRS.14.044501.

18. Diara, F.; Roggero, M. Quality Assessment of DJI Zenmuse L1 and P1 LiDAR and Photogrammetric Systems: Metric and Statistics Analysis with the Integration of Trimble SX10 Data. *Geomatics* **2022**, *2*, 254–281. https://doi.org/10.3390/geomatics2030015.
19. Štroner, M.; Urban, R.; Línková, L. A New Method for UAV Lidar Precision Testing Used for the Evaluation of an Affordable DJI ZENMUSE L1 Scanner. *Remote Sensing* **2021**, *13*, 4811. https://doi.org/10.3390/rs13234811.
20. software, G. *GPL software, 2021. Cloud Compare. GPL software.*; 2021.
21. Roussel, J.R.; Auty, D.; Coops, N.C.; Tompalski, P.; Goodbody, T.R.; Meador, A.; Bourdon, J.; De Boissieu, F.; Achim, A. lidR: An R package for analysis of Airborne Laser Scanning (ALS) data. *Remote Sensing of Environment* **2020**, *251*, 112061. https://doi.org/10.1016/j.rse.2020.112061.
22. Keren, S.; Svoboda, M.; Janda, P.; Nagel, T.A. Relationships between Structural Indices and Conventional Stand Attributes in an Old-Growth Forest in Southeast Europe. *Forests* **2019**, *11*, 4. https://doi.org/10.3390/f11010004.
23. Team, R.C. *R: A Language and Environment for Statistical Computing*; R Foundation for Statistical Computing: Vienna, Austria, 2023.
24. Jucker, T.; Fischer, F.; Chave, J.; Coomes, D.A.; Caspersen, J.; Ali, A.; Loubota Panzou, G.J.; Feldpausch, T.R.; Falster, D.; Usoltsev, V.A.; et al. Tallo: A global tree allometry and crown architecture database. *Global Change Biology* **2022**, *28*, 5254–5268. https://doi.org/10.1111/gcb.16302.